Flexible Polyimide-Based Intracortical Electrode Arrays with Bioactive Capability

Patrick J. Rousche*, *Member, IEEE*, David S. Pellinen, *Student Member, IEEE*, David P. Pivin, Jr., *Member, IEEE*, Justin C. Williams, Rio J. Vetter, and Daryl R. Kipke, *Member, IEEE*

Abstract—The promise of advanced neuroprosthetic systems to significantly improve the quality of life for a segment of the deaf, blind, or paralyzed population hinges on the development of an efficacious, and safe, multichannel neural interface for the central nervous system. The candidate implantable device that is to provide such an interface must exceed a host of exacting design parameters. We present a thin-film, polyimide-based, multichannel intracortical Bio-MEMS interface manufactured with standard planar photo-lithographic CMOS-compatible techniques on 4-in silicon wafers. The use of polyimide provides a mechanically flexible substrate which can be manipulated into unique three-dimensional designs. Polyimide also provides an ideal surface for the selective attachment of various important bioactive species onto the device in order to encourage favorable long-term reactions at the tissue-electrode interface. Structures have an integrated polyimide cable providing efficient contact points for a high-density connector. This report details *in vivo* and *in vitro* device characterization of the biological, electrical and mechanical properties of these arrays. Results suggest that these arrays could be a candidate device for long-term neural implants.

Index Terms—Bioactive device integration, Bio-MEMS, micromotion, neural interface, neuroprosthetics, polyimide.

I. INTRODUCTION

CONTINUED technical advances in the biological, materials and electronics fields have fueled a steady advance in the development of neural interfaces since the advent of the simple intracortical single microelectrode four decades ago. Advanced devices available for implantation into the brain today have multiple electrode sites, are chronically implantable, and can include circuitry for on-board signal processing [1], [2]. Such complex structures are ideal for many potential clinical and basic research applications. For example, there is continuing evidence that a neural interface providing reliable and stable long-term implant function could be used for the realization of clinically useful cortical prostheses for the blind [3], [4]. In addition, the utility of multielectrode arrays has already been demonstrated in basic research studies which have provided fundamental insights into parallel processing strategies during sensory coding in the brain [5]. However, the complex neural interfaces available today have yet to demonstrate the necessary longevity required to support greater strides in the basic neurophysiological research or clinical neuroprosthetic fields. Only when electrode systems can be made to function reliably and consistently for the lifetime of an implanted subject, will these gains be possible.

Development of the first single penetrating microelectrode device spawned the first of three generations of intracortical neural interfaces. In the first generation, microelectrodes simply consisted of known electrically conductive materials that were stiff enough to be inserted through the pia or the dura without buckling. Still in use today, these are as simple as a stiff and sharpened insulated metallic wire, or a drawn glass pipette filled with an aqueous conductor. Due to their high impedance and small site sizes, in order to be effective, these electrodes must be rigorously positioned near their target neurons using precision micromanipulation. Recordings can only be held for several minutes to several hours before repositioning is required. This drawback reduces the attractiveness of this technique for long-term chronic implant. These first generation devices have been upgraded and researchers now routinely employ multiple single microelectrodes aligned into arrays to provide ever-increasing numbers of electrode sites in one device. Some of these devices have positionable electrodes [6]–[8], while others have modified single electrodes (with larger site sizes and/or reduced impedances) which are capable of recording neural activity without precise positioning [9], [10]. These devices can remain functional upon implant for one to twelve months, but the same individual neurons can not be "tracked" longer than about six weeks [9], [10].

Complex electrode designs allowing for batch fabrication of multiple-site devices can be considered as part of the second generation of implantable neural interfaces. These usually monolithic, multisite devices have the capability for integrated electronics and cabling and are created by incorporating planar photolithographic and/or silicon micromachining manufacturing techniques from the electronics industry. Devices intended for recording or stimulation of the cerebral cortex have been created from silicon, [2], [11], [12], or incorporate molybdenum [13]; materials that are stiff enough to penetrate the pia upon implantation. Like first generation devices, these intracortical interfaces can remain patent in the brain for extended time periods, but recording quality and electrode yield typically diminish with time [14], [15].

Other devices are polyimide-based and have been designed to provide a conformal coverage when placed upon the curved
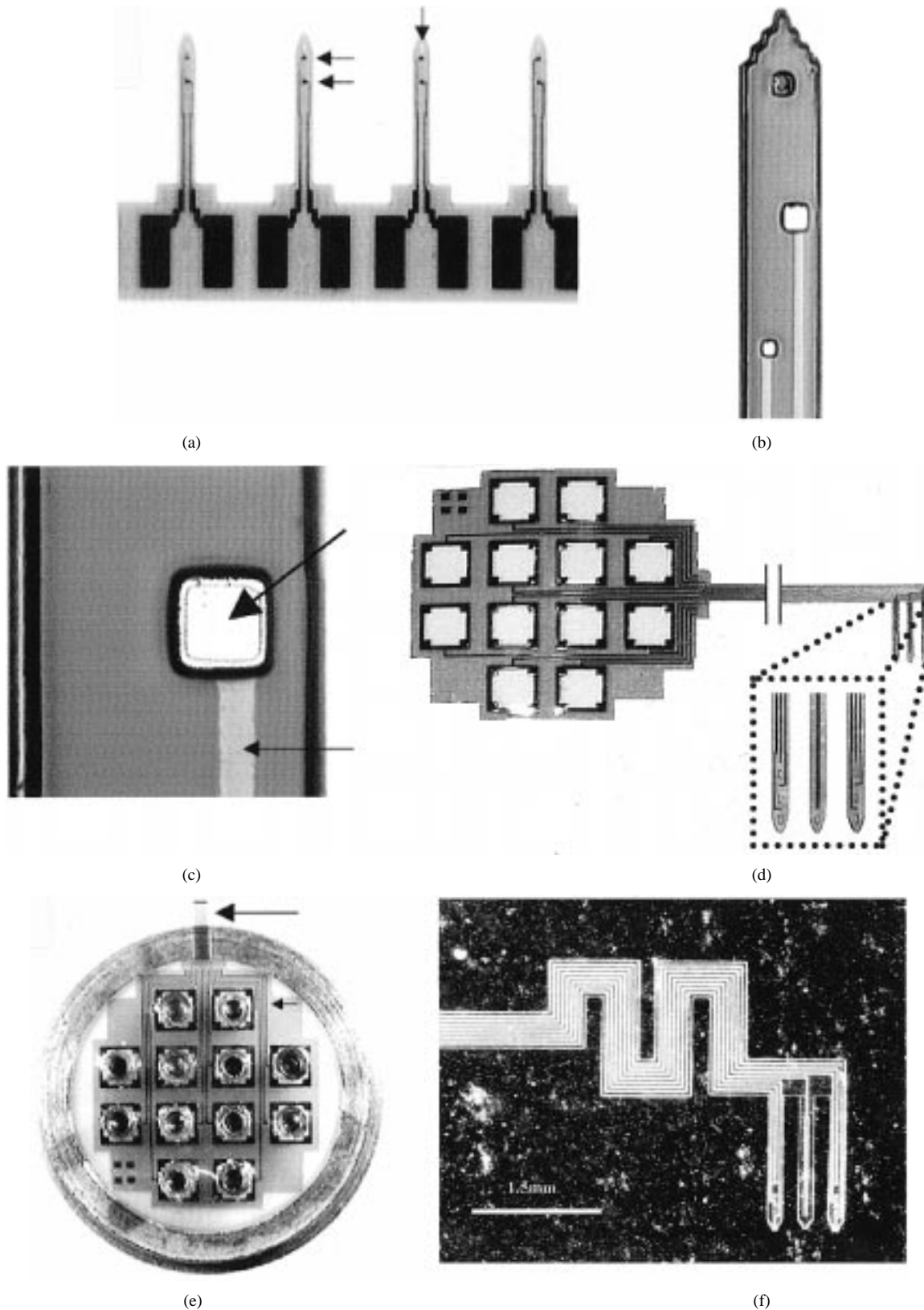
(a)

(b)

(c)

(d)

(e)

(f)

Fig. 1.   A chronically implantable polyimide-based "flexible" intracortical electrode array. (a) Top view of an early four-shaft device. In this device, there are two electrode sites per shaft (double arrows) and a single via (single arrow) at the tip (for tissue integration and bioactive "'seeding"). (b) A close-up view of a single shaft showing a single via and two electrode sites of different sizes (20 × 20 um and 40 × 40 um). (c) The larger site in (b) magnified, showing the exposed gold metal pad (large arrow) and the insulated gold trace (smaller arrow). (d) Complete three-shaft (lengths are 1.5 mm each) device with integrated polyimide cable and simplified feedthrough interconnect system. Inset shows close-ups of the three shafts with exposed electrode sites and vias. One shaft has only a single large ground plane. (e) The interconnect system in place on the backside of a 12-pin Microtech connector. The integrated polyimide cable (large arrow) leads from the device, while the single traces (small arrow) break out to individual connector posts. Conductive epoxy (not shown) is used to provide a consistent electric connection from device to connector. (f) A six-site, three-shaft device with an "S"-curve for strain relief engineered directly into the cable (scale bar lower left = 1.5 mm.) The shafts would be bent at 90° for implant and the cable would run along the surface of the brain to the mounted connector.
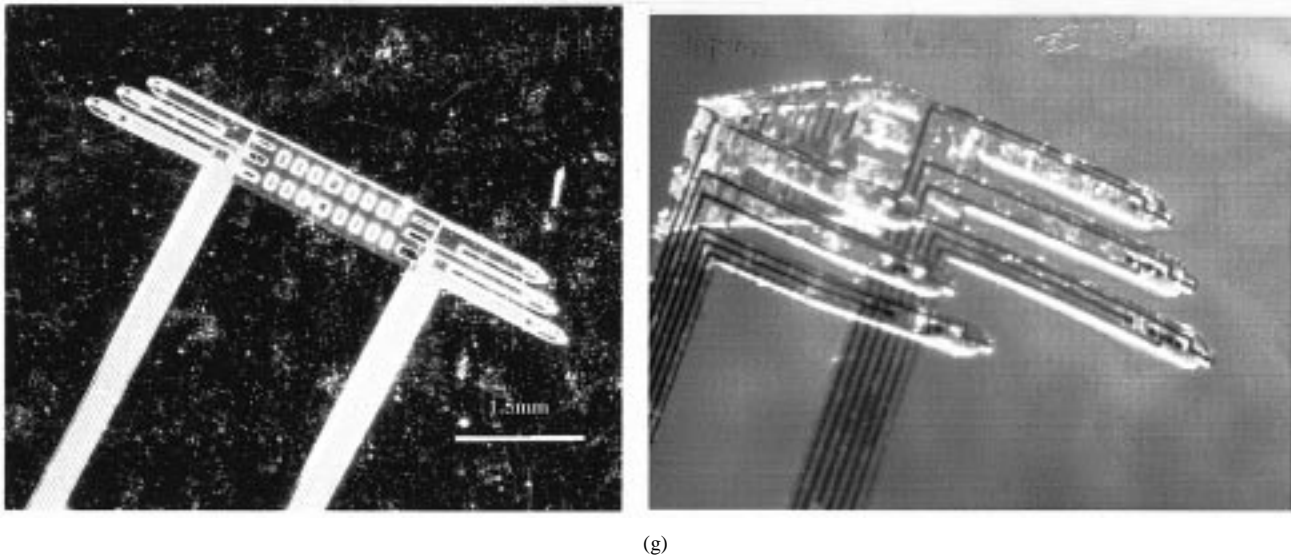
(g)

Fig. 1.   A chronically implantable polyimide-based "flexible" intracortical electrode array. (g) A 2-D structure (scale bar lower right $= 1.5$ mm) and a similar structure "bent" into a 3-D configuration. Only the shafts would be implanted into the cortical mantle. This capability provides a mechanism to create a wide range of devices capable of contacting many neurons within a localized volume depending on shaft size and design.

surface of the brain [16], [17], however, many applications require electrodes to be implanted *into* the cortex.

In the last decade, a third generation of implantable neural interfaces has developed. These latest intracortical electrodes incorporate "bioactive" components. These electrode designs use standard electrically conductive materials in combination with biologically active species in an effort to improve the performance and function of the neural interface. By "seeding" a nontraditional glass microelectrode tip with the active biospecies nerve growth factor (NGF), Kennedy *et al.* have succeeded in creating a neural interface which actively promotes neurite growth toward the recording site [18]. The so-called "cone electrodes" are only single-channel devices, but their efficacy is remarkable. Signal-to-noise ratio (SNR) of the recorded signals are 5–10 times those found in second generation devices. The signals remain stable over extended implant durations (up to 328 days) [19], [20].

In this report, a new class of chronically implantable intracortical electrode arrays which have been expressly designed to meet the exacting design parameters are introduced. The new structures consolidate and incorporate the most desirable aspects of first, second and third generation neural interface devices. Electrode sites of these devices are gold pads (making these preliminary devices suitable for neural recording only), with gold traces (leading to a connector) sandwiched in a mechanically flexible and electrically insulating polyimide substrate. They are manufactured using standard planar photolithographic techniques. The flexibility of the polyimide is intended to provide strain relief against the forces of "micromotion" between the tissue and the implanted device. In addition, the polyimide surface chemistry is amenable to modifications and preparations which allow a host of bioactive organic species to be either adsorbed or covalently bonded to its surface. Device flexibility and bioactivity are intended to provide an optimal implant environment and extend the longevity of the tissue-electrode interface.

Polyimides with acceptably low gas permeability and vapor-transmission rates are obtainable through custom-manufacture [21]. Overall, polyimide is a proven biocompatible material, and an excellent choice for neuroprosthetic applications [22], [23]. This is the first report of a flexible, bioactive, polyimide device designed for long-term *chronic* and *intracortical* use (although electrodes for cortical surface recording [16], [17] and acute "depth" recording [24], have been constructed with similar technology.) Other polyimide devices have been designed for peripheral nerves or muscles [22], [25]–[28]. The standard photolithographic techniques allow for extended design manipulation and prototyping capability with excellent turn-around time ($<$ one week). *In vivo* and *in vitro* data is presented which suggests that these structures provide a promising alternative for an implantable multielectrode system which might remain patent and stable for many years.

II. MANUFACTURING TECHNIQUES

Electrodes were constructed by surface micromachining photosensitive polyimide and gold/chromium metal layers on top of oxidized silicon wafers. Similar types of structures and processes have been previously reported [16], [17], [24], [27], [28]. The structures described here were designed for maximum flexibility. In Fig. 1 several array configurations are presented. Each shaft of earlier structures terminated in bond pads; later designs have an integrated polyimide "cable" terminating in a simplified feed-through interconnect system for attachment of an external connector. Future designs may involve hybrid integration of silicon chips or discrete components for pre-processing or telemetry. In general, the manufacturing process was designed to be as compatible as possible with CMOS processing schedules and equipment to allow future incorporation of monolithic active thin-film transistor circuitry directly onto the probes. A variety of passive array designs have been fabricated to date. Most devices have been single- or tri-shaft devices with electrode site sizes of 20–40 μm $\times$ 20–40 μm and shaft length of
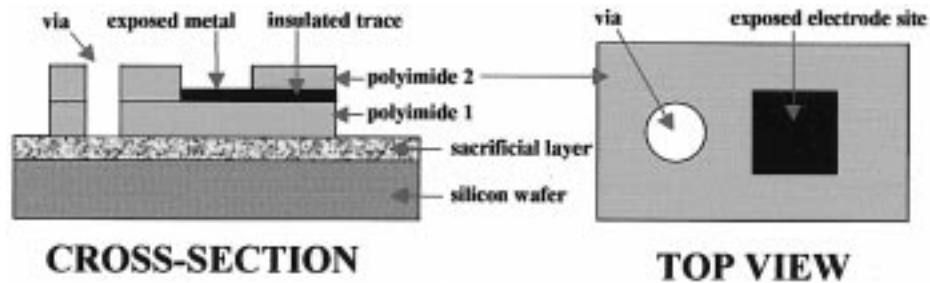
Fig. 2. Schematic views (not necessarily to scale) of the layered construction used in the manufacture of a polyimide electrode array. A single-electrode site (in black) and an accompanying via (or well, in white) are shown. Bioactive species can be selectively pipetted into the via to provide neural in-growth toward the local electrode site region.

1.5 mm. Preliminary three-dimensional (3-D) structures have been created by appropriately placing bends in suitable two-dimensional (2-D) planar structures (see Fig. 1(f)). For all devices, shaft width is 160 μm and thickness is <20 μm. Some devices have been created with "wells" situated 40 μm from each recording site. Essentially vias in the polyimide, these wells are designed to be seeded with bioactive species and provide a route for tissue integration of the device after implant.

A three mask (5-in glass plates with photoactive emulsion or chrome) photolithographic process was used to pattern the layers of polyimide and metal (Au/Cr) into working planar structures. The process begins with bare 4-in silicon wafers, cleaned and etched in a 80 °C, 4:1 solution of H_2SO_4 and H_2O_2. A sacrificial release oxide of 0.5 μm is grown on the surface by wet thermal oxidation. The first layer of photo-active polyimide (Probimide 7520, Arch Chemicals, Norwalk, CT) is then spin coated onto the surface to a thickness of 10–20 μm. This layer of negative photo-active polyimide is exposed and developed using standard photolithography techniques to define the base of the implant structure. The base polyimide layer is then partially cured for 15 min at 350 °C in a nitrogen purged oven to protect the developed pattern from subsequent processing steps and provide a suitable surface for metal deposition.

A reactive ion etch (100 mtorr of O_2 at 50 W for 1 min) is used to micro-roughen the polyimide surface prior to depositing the metal layers. A thin layer of chromium (250 Å) is then electron-beam evaporated onto the wafer to serve as an inter-metallic adhesion promoter. A layer of gold (platinum or iridium may be used as well) 200 nm thick is next evaporated onto the wafer surface. Positive photoresist is patterned over the metal to delineate the individual recording pads, connecting rings and wire traces. Excess metal from the wafer is etched away using Au mask etch (10 g KI, 2.5 g I_2, 100 ml H_2O) for gold and chrome etch solution (1:3 [50 g NaOH + 100 ml H_2O]: [30 g $K_3Fe_9CN)_6$ + 100 ml H_2O]) for chromium.

Another reactive ion etch (100 mtorr O_2 at 50 W for 1 min) is used to clean and micro-roughen the polyimide/metal structures prior to applying the top layer of photo-active polyimide. The top layer of photo-active polyimide is spun on to the same thickness as the base. This layer is then exposed and developed to encapsulate or reveal the desired conducting surfaces. The electrode structures, while on the wafer, are then fully cured (350 °C for 1 h) to complete the imidization process, leaving the structures in their final state. Polyimide shrinks vertically by about

40%–50% during the curing process, leaving the final polyimide structures less than 20 μm thick. The electrode structures are released from the wafer substrate by dissolving the sacrificial oxide in a hydrofluoric acid solution. Several rinses with de-ionized water are then used to remove any unwanted etchant products from the released devices. A cross-sectional schematic diagram of the manufacturing process is shown in Fig. 2. Cytotoxicity tests (LIVE/DEAD Viability/Cytoxicity Test Kit (L-3224), Molecular Probes, Inc., Eugene, OR) on completed polyimide structures alone revealed no significant cytotoxicity among the device materials.

The released electrodes are next fitted onto connectors, with the exposed metal contact rings of the interconnect area facing outward as the male connector pins are pushed through the contact rings. Both 12-pin Microtech, Inc. (Boothwyn, PA- part # FR-12S-4) and 18-pin Omnetics Inc (Minneapolis, MN—Nano series, part # A7855.) connectors have been used. A small amount of conductive epoxy (Chemtronics, Kennesaw, GA, part # AB-5000) is applied between each connector pin and its associated ring to complete the electrical connection. [See Fig. 1(e).] A layer of PMMA (polymethylmethacrylate) dental acrylic is applied to the connector region for insulation, shielding the epoxy from contact with tissue. This same material will eventually be used to bond the electrode to the skull. The feed-through interconnect system significantly reduces the labor required to bond the structure to a connector for chronic implantation.

III. ELECTRICAL, MECHANICAL AND BIOLOGICAL CHARACTERISTICS

Devices intended for successful long-term implant in the nervous system must meet a strict series of criteria in the electrical, mechanical and biological arenas. Electrically, devices must maintain their appropriate insulating and conductive properties over extended implant durations in a saline environment. Mechanically, devices must be capable of withstanding any possible micromotion between tissue and device following implantation. Biologically, as a minimal requirement, the device must maintain a biocompatible profile that does not induce an excessive foreign body or immune response. Even more desirable would be a device capable of inducing useful and supporting positive biological responses such as neurite growth toward the electrode sites. *In vivo* and/or *in vitro* device characteristics in each of these three areas are described below.
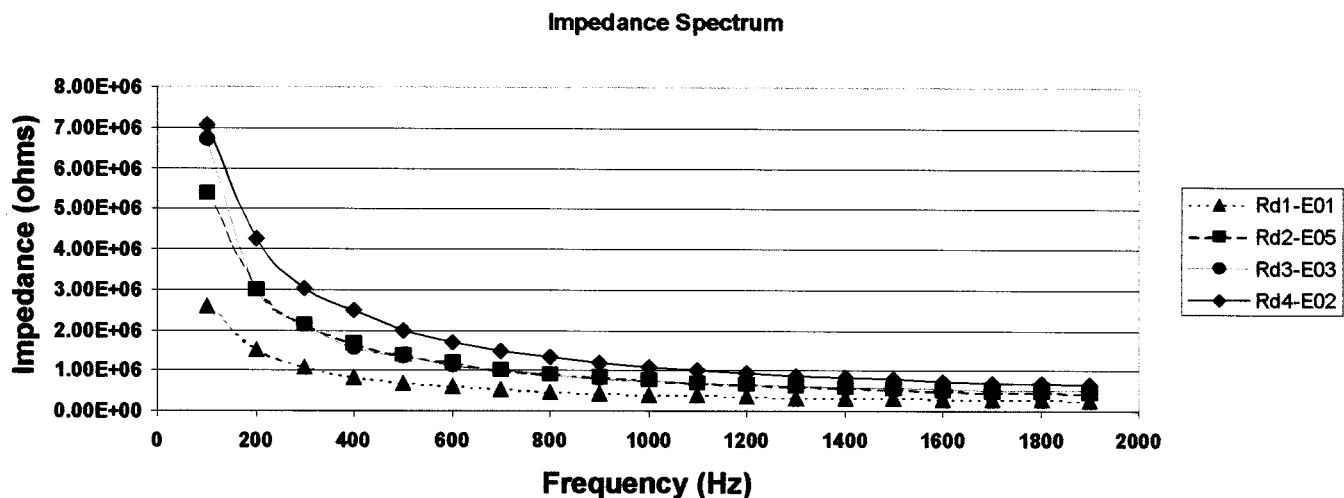
Impedance Spectrum

Fig. 3. Average complex impedance values recorded from four polyimide electrode arrays (six sites per device, 20 readings per frequency) 24 h following chronic implant in the somatosensory cortex of rats. Measurement error bars are smaller than symbol size and thus not shown. Typically, impedances are reported only at the 1-kHz test frequency.

A. Electrical Characteristics

Basic polyimide electrode-cable assemblies were tested in saline before implantation. Impedance measurements were made using a model 4284A Precision LCR meter (Hewlett Packard Co., Palo Alto, CA) which allows for the assessment of complex impedance (resistance, reactance and capacitance) over a large testing frequency range (from 1 Hz to 2 MHz at 5 mV). Saline tests were performed by immersing the shafts and connecting cable of the devices into a 0.9% saline solution at room temperature in a holding chamber sealed from room air. For a single 30×30 μm site from each of four devices tested, average initial complex impedance at the standard frequency of 1 kHz was 1837 ± 197.3 kΩ (one standard deviation) in saline. This value decreased to an average of 355.75 ± 307.5 kΩ following two days of soaking. Despite this initial decrease, impedance remained generally stable over several weeks. This initial drop is likely a result of fully curing the base polyimide layer during preliminary processing. Fully curing the bottom polyimide leaves no un-terminated bonds for attaching the upper polyimide. This may provide a direct route for water vapor transmission through the structure at the double-polyimide layer boundary. On subsequent structures, the base polyimide layer was initially only partially cured, leaving some unconnected terminations in preparation for bonding with the upper polyimide layer. Later structures with a partially cured base show no evidence of early impedance drops.

Four earlier devices were implanted chronically into four separate rat somatosensory cortices and impedance values tested 2–24 h post-implant (see Section IV for surgical details). These particular structures had 3, 1.5 mm length shafts per device, with three sites (30×30 μms each) per shaft on two shafts (the third shaft had a 1000×50-μm site used for an extended ground plane). Testing at the standard 1-kHz frequency revealed the average electrode site impedance (six sites per device, 24 sites total) to be 190.3 ± 25.8 kΩ 2 h following implant. Impedance testing was performed over the entire low-frequency spectra from 100 to 1900 Hz. Fig. 3 displays the averaged (six sites

per measurement point) complex impedance curves for each implanted device recorded 24 h post-implant.

B. Mechanical Characteristics

The devices described in this report have been purposely designed and manufactured to exhibit a mechanical flexibility which is not afforded through the use of "traditional" electrode array materials. Polyimide is an ideal device substrate, as it provides both flexibility and ease of manufacture through standard photolithographic techniques. The mechanical characteristics of the intracortical polyimide electrode arrays were investigated using three mechanical tests, indentation, buckling and extended flexing. Indentation test data were used to calculate the estimated modulus of elasticity of the polyimide arrays. Buckling and flexing tests were used to probe the mechanical viability of the structures through a "before and after" impedance measurement. Devices unaffected by mechanical manipulations should exhibit the same impedance before and after the mechanical disturbance.

1) Indentation: Indentation testing was used to calculate an effective modulus of elasticity for the polyimide devices. Measurements were performed on a nano-indenter (an Atomic Force Microscope (AFM), Hysitron, Minneapolis, MN), with a nano-indentation tip (#10, diamond.) The sample to be tested was fastened to a mounting disk (15 mm in diameter and 5 mm thick) with epoxy bond glue. The sample and disk were then mounted onto the AFM base. The tip was lowered until contact with the sample was made. The load on the tip and hence the sample was determined. The load was cycled linearly from 0 μN to 250 μN to 0 μN over 5 s. Contact depth, maximum load, slope, contact area, maximum depth, effective depth, the reduced modulus of elasticity and the hardness were logged directly or computed. Testing was completed at eight random points on a single device. A calculated modulus of elasticity of 2.793 GPa was obtained. (see Appendix I for details).

2) Buckling: Buckling tests were performed using a microdrive (movement resolution of 10.0×10^{-6} m/step) to hold a single-shaft structure. The structure was lowered perpendicular
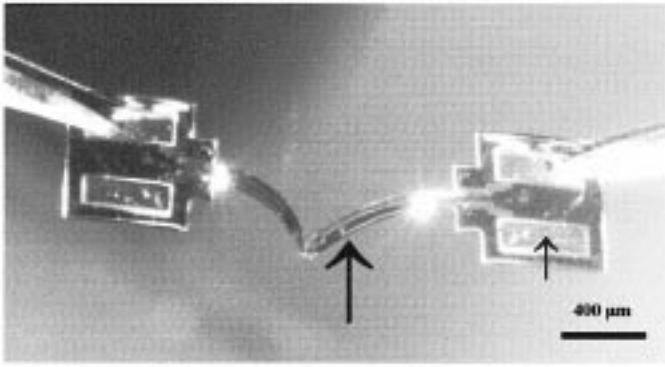
Fig. 4. View of a prototype single-shaft PI electrode array without an integrated cable "flexed" against a mirrored surface. Large arrow points to one of two electrode sites at a trace termination point and small arrow points to an exposed gold bond pad. Black scale bar in lower right corner is 400 μm.

to a model AE 160 force scale (Mettler-Toledo Inc., Columbus, OH) until contact was achieved. Initial buckling force loads were determined from the scale reading taken when visual observation confirmed that the structure had buckled. As an example, Fig. 4 shows a structure flexed far past the minimum buckling point. Measurements were repeated five times for five different single-shaft structures. The mean value of buckling force load was calculated to be 0.00362 ± 0.000628 N. Theoretical buckling force load for a polyimide structure of this size and length 0.00250 N. See Appendix I for details.

3) Extended flexing: To test the ability of the polyimide electrode arrays to withstand varying mechanical traumas, devices were continuously and repeatedly flexed using a custom made apparatus. Single-shaft devices were positioned within the path of a 2.54-cm diameter plastic microgear wheel (tooth separation of 1.5 mm) in room air. A 40-Hz sinusoidal input to the gear wheel provided a continuously reversing mechanical stimulus. Shaft flexion of about 45° was obtained as each of two neighboring gear teeth pressed against the flexible shaft in succession. Impedance measurements in saline were taken from 18 electrode sites on three different devices before and after at least one million of these mechanical disruptions in each direction. Average percent change in impedance after mechanical manipulations were -8.37%, $+2.43\%$ and $+9.31\%$ per device (six sites per device). These results suggest that extended flexing does not induce mechanical breakdown of the conductive traces or electrode sites. Likewise, anecdotal evidence of soak-tested structures suggests that impedance in saline does not change even after permanent 90° bends (with a minimal radius of curvature) are placed into the structures.

C. Biological Characteristics

A major promise of polyimide as the insulating substrate for a neural implant is the amenability of its surface chemistry to the attachment of biological species. Bioactive components can be incorporated onto the polyimide surface through simple adhesion or through covalent bonding (with appropriate surface modification). By selectively applying various bioactive species to different segments of polyimide devices, structures can be engineered for maximum *in vivo* performance. The bioactive compounds can be delivered via a variety of carriers. In Fig. 5, one
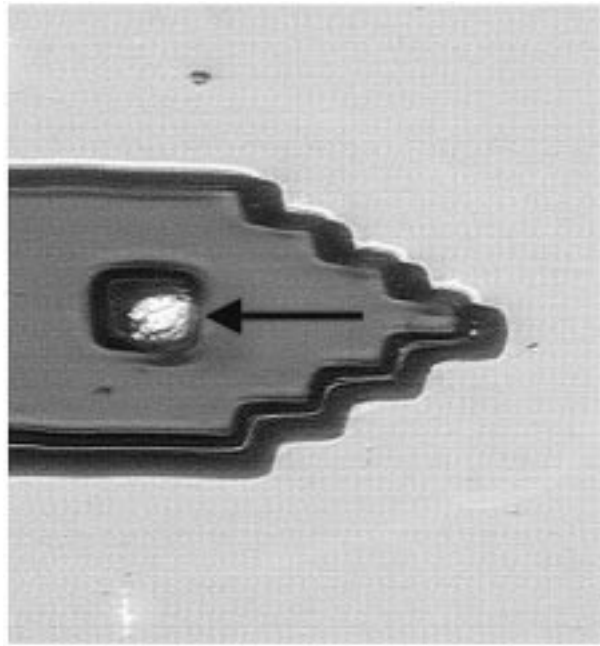

Fig. 5. A via or "well" in a polyimide electrode array (100×50 μm) selectively filled with a dextran hydrogel (arrow). The gel can be seeded with any number of useful bioactive species such as NGF. By filling a variety of wells with a variety of bioactive components, intracortical polyimide devices can be engineered for maximum biological acceptance. A micropipette system is used to fill the wells.

well from the end of a typical three-shaft structure is shown in which the well has been preferentially "seeded" with a dextran gel. Seeding is accomplished by microinjection of the gel into the well. The process uses a micropipette that has been pulled to approximately a 10-μm outer diameter (custom-sized to the well dimensions), so that the end of the pipette fits inside the well. The pipette position is controlled with a microinjection system (Patchman and Transinjector 5246, Eppendorf - Netheler - Hinz GmbH, Hamburg, Germany) under a microscope. Starting at one end, the pipette is drawn along the inside surface of the well, allowing capillary action to fill the well. After the well is completely filled, the pipette is repositioned in the center of the well and slowly advanced out of the well, applying a slight suction on the pipette to prevent surface tension from pulling more gel out of the pipette and onto the outside polyamide surface. Other devices have been nonselectively coated using a fibrin gel, which can be used as an alternate carrier of bioactive species.

IV. RECORDING CAPABILITY

Flexible and bioactive electrode probe structures may provide the critical technological break-through that allows for the long-term neural recording and stimulation of large groups of the same neurons feasible. To date, only limited success has been reported in the development of a system capable of maintaining a stable long-term interface. It is not the purpose of the present report to demonstrate long-term performance of the polyimide intracortical electrode array; a companion report will address that topic. However, in this report, the short-term chronic recording capability of the polyimide structures is demonstrated. We show that these devices, when properly

configured, are capable of chronically recording multiunit neural activity with reasonable SNRs in the rat barrel cortex.

A. Implantation

Rats were anaesthetized with a ketamine-xylazine-aceproza-mine mix. Heart rate and oxygen saturation were monitored throughout the sterile procedure. A 4 × 4 mm craniotomy was performed to expose S1, the rat somatosensory cortex containing the whisker representation (barrel cortex). Traditionally, stiff electrodes for cortical implant are lowered to the surface and entered into the cortical mantle through the dura and pia, or the dura is removed and the electrodes lowered through the pia alone. The low buckling force of the polyimide electrode array precludes the use of this implant technique. The electrode shafts will always buckle during the insertion attempt before enough force can be generated to create an incision in the pia. Thus, we have developed and tested an alternate technique to allow for the safe implantation of these flexible devices. Three pial incisions were created (one for each shaft), either with a #11 scalpel, or a relatively stiff 100-μm tungsten wire. The incisions were created to match the shaft spacing pattern. To encourage post-implant recovery, great care was made to ensure that the incisions were made with as little associated tissue damage as possible.

Once the incisions were created, the polyimide devices were inserted. Chronic cable and connector assemblies were first appropriately positioned by permanently mounting the connector "can" onto a nearby section of exposed skull with a small amount of PMMA. The polyimide cable leading from the shafts to the connector was about 1 cm in these devices. Before final cementing of the can however, the electrode shafts were arranged so that they rested "naturally" near the incisions, preferably with an implied "bowing" of the integrated cable to provide additional strain relief to the implanted shafts. The electrode shafts were then inserted en masse, by hand, using a #5 forceps viewed with an operating microscope. The devices slipped very easily into the cortical mantle through the pial incisions only when appropriately aligned. More complex designs incorporating more shafts will require alternate methods for holding and lowering the device. After implant, the protruding cable and any exposed pia were packed with small pieces (1 × 1 mm) of GelFoam (Pharmacia and UpJohn, Peapack, NJ). A final layer of PMMA was applied over the GelFoam mound, sealing the craniotomy. Two external grounds were provided by stainless steel wires attached to two implanted stainless steel bone screws (size 00-80).

Recordings were performed in still anaesthetized and in fully awake animals using a Plexon Inc. (Dallas, TX) MNAP system. Signals were buffered with a headstage unity-gain FET amplifier system, then amplified from 20 000–30 000 times and filtered from 300–5000 Hz. Multiunit neural activity indicative of barrel cortex under anesthesia and in the awake state was recorded [29]. In Fig. 6, periodic multiunit firing induced by manual contralateral whisker stimulation over a 6-s period is presented 24 h post-implant. The stimuli is simply a repeated manual stimulation of the full whisker set using the wooden shaft of a cotton-tipped applicator. Maximum signal amplitude
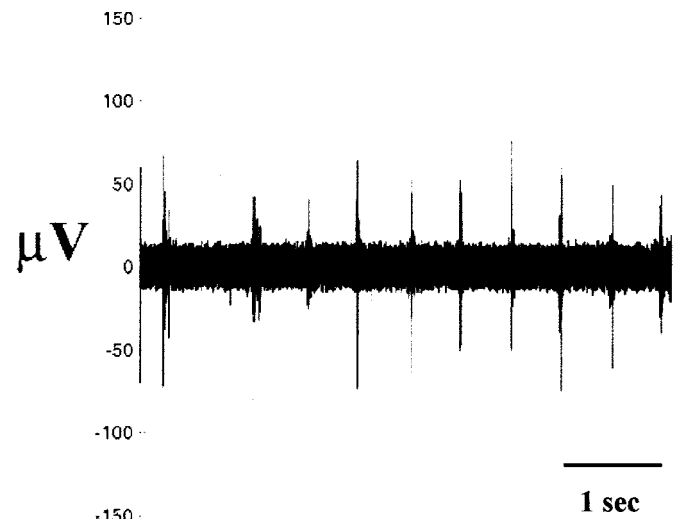

Fig. 6. A continuous six second sample showing multiple unit activity recorded from rat whisker barrel cortex from one site of a polyimide electrode array (site size 40 × 40 um). Stimulus (not shown) was a repetitive manual activation of the contralateral whiskers.

resulting from this stimulus is about 150-μV peak-to-peak and the maximum SNR is roughly 5:1.

V. DISCUSSION

A multichannel neural interface for long-term recording or stimulation (with modifications) in the cerebral cortex has been described. The device is manufactured in-house in a Class 100 clean room on 4-in silicon wafers using planar photolithographic manufacturing techniques. Composed of gold electrodes sandwiched in a flexible bi-layer polyimide insulating substrate, the array is capable of sensing multiunit neural activity from cerebral cortex. Mechanical, electrical, and biological characteristics of the device support the assertion that this device could be a candidate for extended implant applications in the brain. Extremely stable neural interfaces which maintained contact with sets of the same neurons for years would be advantageous both for advancing the basic understanding of normal brain function, and for implementing neuroprosthetic clinical applications such as a motor prosthesis based on cortical recordings or a visual prosthesis based on cortical microstimulation. The device has been expressly designed to meet the exacting specifications required by such advanced uses. In designing a neural implant capable of meeting the rigorous design specifications detailed in the Introduction, the first challenge was to choose an appropriate biocompatible material. Polyimide is a demonstrated biocompatible material [23] with the capability to support the incorporation of on-board circuitry (not explored in this report). The use of polyimide provides several other advantages and mechanisms by which the design specifications can be met. Three main advantages of polyimide are discussed below.

A. Mechanical Features

Traditionally, electrodes have been constructed using materials known to have excellent electrical properties, with little re-

gard to their mechanical properties. Metal, glass, or silicon electrodes all can function extremely capably as neural interfaces, but these materials are generally stiff. Stiff materials create a mechanical impedance mismatch when interfaced with the relatively viscous environment of the neural tissue.

Polyimide was chosen for this device because of its inherent flexibility. In planar form, the flexibility is evident in motions orthogonal to the plane of the structure. A device that moves with the brain tissue would be much less susceptible to the problem of micromotion, a problem that confounds stiff implants [30]. The flexibility of the polyimide array could provide a significant defense against micromotion, but additional testing will be required to determine if its conditional flexibility in the manufacturing plane is enough to enhance long-term performance. Certainly, the results of the extended flexing experiments verify that polyimide is capable of long-term mechanical variations without any degradation in electrical performance of the electrode sites or cables. These tests stressed the polyimide structures more than a million times in opposite directions much further than is likely to occur *in situ*. Flexibility is also a key feature that is employed in the manufacture of complex 3-D structures. These structures, introduced in Fig. 1(e), require precise 90° bends of an originally planar substrate. When performed carefully, these bends do not cause structural damage or interfere with the electrical conduction (impedance measurements of saline-soaked structures before and after the bend remain constant).

Another unique feature of polyimide is its ability to be easily mechanically reworked using a variety of photolithographic techniques or an excimer laser [31]. With these processes, small controlled microlesions of the polyimide surface can be formed. The creation of local pits or grooves can be used to provide a device with a jagged surface profile more amenable to the biological environment. Similar modification of silicon structures have been shown to significantly decrease protein adsorption over smooth, un-worked structures upon implant into biological tissue [32]. In addition, the excimer laser can be used to completely ablate small areas of polyimide within the structures. Dispersed throughout the polyimide structure (but avoiding the electrode sites and traces toward the connector), these via holes would provide a more minimal interruption of the cortical mantle and possibly encourage rapid astrocyte re-growth through the implanted structure. This re-growth might better stabilize the implanted device.

B. Bioactive Capability

In the brain, only one chronically implantable device to date has incorporated bioactive coatings. Kennedy *et al.* have successfully demonstrated that a single electrode in the brain seeded with NGF can remain patent and provide very usable neural signals. The addition of the NGF dramatically improves SNR, and enhances long-term performance (the latest report showed a human implanted with a single electrode still functioning 328 days post-implant) [19].

Another advantage in choosing polyimide as the device substrate is the ability to attach such important biological entities to the surface. In Fig. 5, wells placed near recording sites were shown "seeded" with significant concentrations of
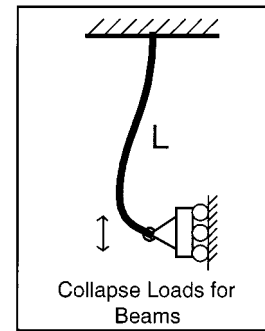

Fig. A1. Inverted schematic mechanical representation of the single-shaft polyimide device (length $L = 1.5$ mm) used for calculation of theoretical critical load for buckling. One end of the shaft is completely pinned.

NGF. By placing and seeding wells near each recording site, we intend to encourage neurite growth toward each active electrode. Like the cone electrode, such growth should boost the SNR and provide a more stable interface. The polyimide array however, would provide a far larger number of active electrode sites than the single-electrode Kennedy device. Attached biomolecules would not need to be limited to NGF. Any appropriate species which could successfully influence the integrity of the tissue-electrode interface can be considered. For example, species which inhibited capsule formation might be equally useful in providing an ideal environment for the neural interface. Further experiments will determine the efficacy of various selectively applied bioactive coatings.

C. Rapid Prototyping

An invaluable advantage in creating a device rigorous enough to be considered a candidate for long-term implant durations is that of rapid prototyping. Electrode design, manufacture and testing can be a lengthy, laborious and expensive operation. Polyimide can be processed using standard planar photolithographic techniques on 4-in silicon wafers. While not necessarily inexpensive, this design process does allow for quick turn around on new designs. Full production of each device set takes roughly two-three days. Completion of mask design and generation may take several more days depending on the pattern complexity. This relatively short time period allows for the efficient assessment of many design parameters, such as device shape, thickness, width, electrode site size, etc. Rapid prototyping also ensures that devices can be custom-tailored to their individual implant requirements. Such factors as implant shape and depth will vary from animal to animal or in various clinical subjects. Thus, rapid prototyping is beneficial both in the development stage and in the production of various differing structures.

VI. Conclusion

A thin-film polyimide-based intracortical electrode array has been introduced. The device has been designed to meet the exacting requirements for a neural interface designed for long-term use in the clinical neuroprosthetics or basic neuroscience fields. Preliminary electrical, mechanical, and biological testing confirm that the new device may have the features required to enhance long-term performance. These

Approximated Dimensions
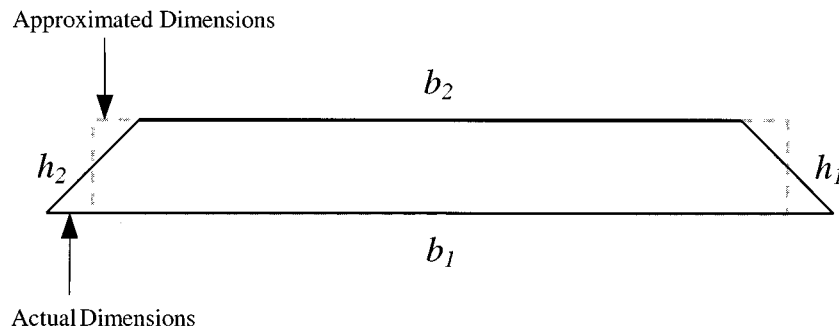
b_2

h_2

h_1

b_1

Actual Dimensions

Fig. A2. Actual cross-sectional dimensions versus approximated dimensions for a single-shaft polyimide device. Approximations are used in the calculation of the theoretical critical buckling load.

include increased mechanical flexibility and bioactive capabilities. Further testing will confirm if these traits are indeed the key to increased performance and functionality.

APPENDIX I

Variables

E_p	modulus of elasticity of polyimide (GPa);
E_r	reduced modulus of elasticity (GPa);
E_i	modulus of elasticity of indenter (GPa);
v_i	Poisson's ratio of indenter;
v_p	Poisson's ratio of polyimide;
I_m	moment of Inertia(m^4);
λ	slenderness ratio;
A	cross-sectional area (μm^2);
b	base length (μm);
h	height length (μm);
r_x	radius of gyration (m);
L_e	effective length (mm);
P_{cr}	critical load (N);
K	effective length constant.

Calculation of the theoretical critical load which induces buckling for a single-shaft polyimide electrode array is presented here. E_p, the modulus of elasticity of the polyimide structure, was obtained for these calculations using an atomic force microscope (E_p = 2.793 GPa). P_{cr}, the critical load which induces buckling, was then determined using Euler's buckling force equation, (P_{cr} = 0.002 50 N).

E_p was determined by indenting the polyimide structure with the atomic force microscope tip and measuring the resulting mechanical deformation to obtain a reduced modulus of elasticity, E_r. E_r was then used to calculate E_p = 2.793 GPa as follows (see [33]):

$$\frac{1}{E_r} = \frac{1 - v_p^2}{E_p} + \frac{1 - v_i^2}{E_i}$$

where

E_r	3.1495 GPa (measured via AFM);
E_i	1140 GPa (AFM specifications);
v_p	0.34 (Olin Microelectronic Materials, Norwalk, CT);
v_i	0.07 (AFM specifications).

Euler's buckling force equation can be only be used if the device falls in the long column class, determined if the slenderness ratio is greater than 120 (see [34].) A slenderness ratio, $\lambda = 127$ was obtained using

$$\lambda = \frac{L_e K}{r_x}$$

where $L_e = L * K$ is the effective length (m) and r_x is the radius of gyration (m^2). An effective length, L_e = 1.05 mm was calculated assuming a "Fixed-pinned Column" with effective length constant of K = 0.699. Fig. A1 (see [34]) shows a schematic representation. A radius of gyration, r_x = 5.77 × 10^{-6} m^2, was calculated using,

$$r_x = \left(\frac{I_m}{A}\right)^{1/2}$$

where A, the cross-sectional area, $= b * h = 3000 \ \mu$m^2, and I_m, the moment of inertia, $= 1.0 \times 10^{-19}$ m^4. I_m was determined using

$$I_m = \tfrac{1}{12}(bh^3)$$

where $b = 150 \ \mu$m and $h = 20 \ \mu$ (the width and thickness of the column, see Fig. A2).

The theoretical buckling force load, P_{cr}, therefore, can be calculated directly using Euler's buckling force equation, resulting in P_{cr} = 0.002 50 N.

$$P_{cr} = \frac{\pi^2 E_p I_m}{L_e^2}.$$

Assumptions

1) The electrode is classified as a "beam" with a length of 1.5 mm.
2) The cross-sectional area of the electrode is assumed to be a rectangle, when in actuality it is a trapezium. The approximated dimensions are $b_1 = b_2 = 150 \ \mu$m and $h_1 = h_2 = 20 \ \mu$m. The actual dimensions are $b_1 = 160 \ \mu$m, $b_2 = 140 \ \mu$m, and $h_1 = h_2 = 28 \ \mu$m.
3) The small mechanical variations added by the very thin traces of gold and chromium existing within the polyimide are neglected.
4) When using the "fixed-pinned column" diagram, it is assumed that the electrode is "fixed" at the top of the shaft,

which excludes all material beyond this point. (i.e., bond pad area, polyimide cable, etc.).

5) When using the "fixed-pinned column" diagram, it is assumed that there is no lateral translation of the electrode at the "pinned" end of the electrode.

6) The shape of the electrode is assumed constant throughout the length we are using to measure the buckling force. The shape change of the electrode as it tapers toward the tip is neglected.

REFERENCES

[1] C. Kim and K. D. Wise, "A 64-site multishank CMOS low-profile neural stimulating probe," *IEEE Trans. Biomed. Eng.*, pp. 1230–1238, 1996.

[2] K. E. Jones, P. K. Campbell, and R. A. Normann, "A glass/silicon composite intracortical electrode array," *Ann. Biomed. Eng.*, vol. 20, no. 4, pp. 423–437, 1992.

[3] E. M. Schmidt, M. J. Bak, F. T. Hambrecht, C. V. Kufta, D. K. O'Rourke, and P. Vallabhanath, "Feasibility of a visual prosthesis for the blind based on intracortical microstimulation of the visual cortex," *Brain*, vol. 119, Pt. 2, pp. 507–522, Apr. 1996.

[4] W. H. Dobelle, "Artificial vision for the blind by connecting a television camera to the visual cortex," *ASAIO J.*, vol. 46, no. 1, pp. 3–9, Jan. 2000.

[5] M. A. Nicolelis, L. A. Baccala, R. C. Lin, and J. K. Chapin, "Sensorimotor encoding by synchronous neural ensemble activity at multiple levels of the somatosensory system," *Science*, vol. 268, no. 5215, pp. 1353–1358, June 1995.

[6] H. M. Sinnamon and D. J. Woodward, "Microdrive and method for single unit recording in the active rat," *Physiol. Behav.*, vol. 19, no. 3, pp. 451–453, Sept. 1977.

[7] H. J. Reitbock and G. Werner, "Multielectrode recording system for the study of spatio-temporal activity patterns of neurons in the central nervous system," *Experientia*, vol. 39, no. 3, pp. 339–341, Mar. 1983.

[8] R. C. deCharms, D. T. Blake, and M. M. Merzenich, "A multielectrode implant device for the cerebral cortex," *J. Neurosci. Methods*, vol. 93, no. 1, pp. 27–35, Oct. 1999.

[9] J. C. Williams, R. L. Rennaker, and D. R. Kipke, "Long-term neural recording characteristics of wire microelectrode arrays implanted in cerebral cortex," *Brain Res. Brain Res. Protoc.*, vol. 4, no. 3, pp. 303–313, Dec. 1999.

[10] M. A. Nicolelis, A. A. Ghazanfar, B. M. Faggin, S. Votaw, and L. M. Oliveira, "Reconstructing the engram: Simultaneous, multisite, many single neuron recordings," *Neuron*, vol. 18, no. 4, pp. 529–537, Apr. 1997.

[11] A. C. Hoogerwerf and K. D. Wise, "A three-dimensional microelectrode array for chronic neural recording," *IEEE Trans. Biomed. Eng.*, vol. 41, pp. 1136–1146, Dec. 1994.

[12] K. D. Wise and J. B. Angell, "A low-capacitance multielectrode probe for use in extracellular neurophysiology," *IEEE Trans. Biomed. Eng.*, vol. BME-22, pp. 212–219, May 1975.

[13] N. A. Blum, B. G. Carkhuff, H. K. Charles, Jr., R. L. Edwards, and R. A. Meyer, "Multisite microprobes for neural recordings," *IEEE Trans. Biomed. Eng.*, vol. 38, pp. 68–74, Jan. 1991.

[14] P. J. Rousche and R. A. Normann, "Chronic recording capability of the Utah Intracortical Electrode Array in cat sensory cortex," *J. Neurosci. Methods*, vol. 82, no. 1, pp. 1–15, July 1998.

[15] E. M. Maynard, N. G. Hatsopoulos, C. L. Ojakangas, B. D. Acuna, J. N. Sanes, R. A. Normann, and J. P. Donoghue, "Neuronal interactions improve cortical population coding of movement direction," *J. Neurosci.*, vol. 19, no. 18, pp. 8083–8093, Sept. 1999.

[16] A. L. Owens, T. J. Denison, H. Versnel, M. Rebbert, M. Peckerar, and S. A. Shamma, "Multielectrode array for measuring evoked potentials from surface of ferret primary auditory cortex," *J. Neurosci. Methods*, vol. 58, no. 1–2, pp. 209–220, May 1995.

[17] S. A. Peckerar, S. A. Martin, and S. A. Shamma, "Passive microelectrode arrays for recording of neural signals: A simplified fabrication process," *Rev. Sci. Instrum.*, vol. 62, no. 9, pp. 2276–2280.9-1, 1991.

[18] P. R. Kennedy, "The cone electrode: A long-term electrode that records from neurites grown onto its recording surface," *J. Neurosci. Methods*, vol. 29, no. 3, pp. 181–193, Sept. 1989.

[19] P. R. Kennedy, R. A. Bakay, M. Moore, K. Adams, and G. Montgomery, "Neural activity during acquisition of cursor control in a locked-in-patient," *Soc. Neurosci. Abstr.*, vol. 25, no. 1, pp. 894–894, 1999.

[20] P. R. Kennedy and R. A. Bakay, "Restoration of neural output from a paralyzed patient by a direct brain connection," *Neuroreport*, vol. 9, no. 8, pp. 1707–1711, June 1998.

[21] H. Kawakami, S. Nagaoka, and S. Kubota, "Gas transfer and in vitro and in vivo blood compatibility of a fluorinated polyimide membrane with an ultrathin skin layer," *ASAIO J.*, vol. 42, no. 5, pp. M871–M876, Sept. 1996.

[22] T. Stieglitz and J. U. Meyer, "Implantable microsystems. Polyimide-based neuroprostheses for interfacing nerves," *Med. Dev. Technol.*, vol. 10, no. 6, pp. 28–30, July 1999.

[23] R. R. J. Richardson, J. A. Miller, and W. M. Reichert, "Polyimides as biomaterials: Preliminary biocompatibility testing," *Biomaterials*, vol. 14, no. 8, pp. 627–635, July 1993.

[24] G. A. Urban, J. A. Ganglberger, F. Olcaytug, F. Kohl, R. Schallauer, M. Trimmel, H. Schmid, and O. Prohaska, "Development of a multiple thin-film semimicro DC-probe for intracerebral recordings," *IEEE Trans. Biomed. Eng.*, vol. 37, pp. 913–918, Oct. 1990.

[25] T. Stieglitz and H. M. J. U. Beutel, "A flexible, light-weight multichannel seive electrode with integrated cables for interfacing regenerating peripheral nerves," *Sensors Actuators*, vol. A60, pp. 240–243, 1997.

[26] T. Stieglitz and J. U. Meyer, "Microtechnical interfaces to neurons," *Microsyst. Technol. Chem. Life Sci.*, pp. 131–162, 1997.

[27] S. A. Boppart, B. C. Wheeler, and C. S. Wallace, "A flexible perforated microelectrode array for extended neural recordings," *IEEE Trans. Biomed. Eng.*, vol. 39, pp. 37–42, Jan. 1992.

[28] C. Gonzalez and M. Rodriguez, "A flexible perforated microelectrode array probe for action potential recording in nerve and muscle tissues," *J. Neurosci. Methods*, vol. 72, no. 2, pp. 189–195, Apr. 1997.

[29] D. J. Simons, G. E. Carvell, A. E. Hershey, and D. P. Bryant, "Responses of barrel cortex neurons in awake rats and effects of urethane anesthesia," *Exp. Brain Res.*, vol. 91, no. 2, pp. 259–272, 1992.

[30] D. J. Edell, V. V. Toi, V. M. McNeil, and L. D. Clark, "Factors influencing the biocompatibility of insertable silicon microshafts in cerebral cortex," *IEEE Trans. Biomed. Eng.*, vol. 39, pp. 635–643, June 1992.

[31] Y. Nakayama and T. Matsuda, "Surface microarchitectural design in biomedical applications: Preparation of microporous polymer surfaces by an excimer laser ablation technique," *J. Biomed. Mater. Res.*, vol. 29, no. 10, pp. 1295–1301, Oct. 1995.

[32] J. Meyle, H. Wolburg, and A. F. von Recum, "Surface micromorphology and cellular interactions," *J. Biomater. Appl.*, vol. 7, no. 4, pp. 362–374, Apr. 1993.

[33] W. D. Pilkey, *Stress, Strain, and Structural Matrices*. New York: Wiley, 1994.

[34] J. Case, L. Chilver, and C. Ross, *Strength of Materials and Structures*. New York: Wiley, 1994.

Patrick J. Rousche (M'00) received the B.S. degree in bioengineering from Syracuse University, Syracuse, NY, in 1989 and the Ph.D. degree in bioengineering from the University of Utah, Salt Lake City, in 1996.

He is currently a Research Assistant Professor in the Neural Engineering Group, Department of Bioengineering, Arizona State University, Tempe. His research interests are primarily in the development and application of multichannel neural interfaces for both applied neuroprosthetics and basic neuroscience.

David S. Pellinen (S'99) received the B.S. degree in electrical engineering from the University of Arizona, Tempe, in 1995. He is currently working toward the Ph.D. degree in bioengineering and the MSE degree in electrical engineering at Arizona State University.

He presently works in the Neural Engineering Group in the Bioengineering Department at Arizona State University. His research areas of interest include biological MEMS and biosensors.

Justin C. Williams received the B.S. degree in mechanical engineering and the B.S. degree in physics from South Dakota State University, Vermillion, in 1995 and 1996, respectively. He is currently working toward the Ph.D. degree in the Department of Bioengineering at Arizona State University. His research interests are in neural interfacing and bio-MEMS.

Rio J. Vetter received the B.S.E. degree in bioengineering from Arizona State University, Tempe. He is currently a graduate student at Arizona State University.

His research is focused on characterizing the recording capabilities and enhancing the electrical performance of electrode arrays for the brain.

David P. Pivin, Jr. (S'89–M'99) was born in Long Beach, CA, on March 8, 1970. He received the B.S., M.S., and Ph.D. degrees in electrical engineering from Arizona State University, Tempe, in 1992, 1994, and 1998 respectively.

He is currently a Research Assistant Professor at Arizona State University, with a joint appointment in the Electrical and Chemical/Materials Engineering departments. His current research interests are in the areas of nanometer-scale fabrication technology and device physics, biological MEMS, and novel sensors and actuators based on mesoscopic interactions. In addition to conducting research in these areas, he oversees a focused ion beam facility within the Center for Solid State Electronics Research.

Dr. Pivin is a member of the American Physical Society and the American Vacuum Society.

Daryl R. Kipke (S'87–M'90) received the Ph.D degree in bioengineering from the University of Michigan, Ann Arbor.

From 1992 to the present, he has been a faculty member in the Department of Bioengineering at Arizona State University, Tempe. His main research interests are bioengineering, bio-MEMS, and systems neuroscience.